Journal of Applied Analysis and Computation
Volume 16, Number 4, August 2026, 2218–2237
Website:http://www.jaac-online.com
DOI:10.11948/20250367

THE INFLUENCE OF SMALL PERMANENT CHARGES AND PARTIAL BOUNDARY CONDITIONS ON INDIVIDUAL FLUXES VIA POISSON-NERNST-PLANCK SYSTEMS

Yiwei Wang[1,2] and Lijun Zhang[2,3,†]

Abstract We investigate ionic flow through membrane channels within a one-dimensional Poisson-Nernst-Planck framework, considering two oppositely charged ion species and incorporating a small but non-zero permanent charge. Building upon prior analysis in [50], which was confined to cases with higher left-side concentrations, we relax this constraint to examine a broader and more physiologically relevant range of boundary conditions. Crucially, instead of considering the product of zeroth- and first-order terms in the flux expansion, we focus on the first-order term itself, which directly captures the leading effects of channel geometry and permanent charge. Under partial electroneutral boundary conditions, our analysis results demonstrate that the permanent charge plays a regulatory role: It can either enhance or suppress both ion fluxes simultaneously, or exert opposing effects by increasing anion flux while decreasing cation flux - an outcome that depends on the electric potential applied at the boundary. We further identify and compare several critical electric potentials, providing new insights into the transport mechanisms operative across different potential intervals. Numerical simulations on selected cases yield results in excellent agreement with the theory, confirming and supporting our analytical conclusions.

Keywords PNP systems, permanent charges, individual fluxes, partial boundary conditions.

MSC(2010) 34A26, 34B16, 34D15, 37D10, 92C35.

1. Introduction

Ion channels are large proteins embedded in the cell membrane with a central pore that provides a regulated pathway for the electrodiffusion of ions (such as Na^+, K^+, Ca^{++} and Cl^-) across biological membranes. They enable communication between cells and their external environment, thereby controlling a wide range of biological functions. In addition to external driving forces, such as boundary electric potentials and ion concentrations, ionic flow through these atomic-scale channels is also influenced by other factors, including the shape of its pore and the distribution of permanent charge along the channel's inner surface [12, 13, 16–18, 22].

Ionic flows follow electrodiffusion laws, where current-voltage relations capture key channel

[†]The corresponding author.
[1]College of Mathematics and Systems Science, Shandong University of Science and Technology, Qingdao, Shandong 266510, China
[2]School of Science, Zhejiang University of Science and Technology, Hangzhou, Zhejiang 310023, China
[3]Material Science, Innovation and Modelling Research Focus Area, North-West University, Mafikeng Campus, Mmabatho 2735, South Africa
Email: yiwei_1223@163.com(Y. Wang), li-jun0608@163.com(L. Zhang)

properties: Permeation and selectivity. However, individual ion fluxes–though rarely measurable directly–provide more functional insight than total current alone [23,29]. Mathematical analysis is crucial to reveal underlying mechanisms, especially when analytical solutions are attainable. Recent advances in Poisson-Nernst-Planck (PNP) models [2,6–8,11,14,15,25,29,31,33,34,38–41, 43,47,48,52] have greatly improved our qualitative understanding of flow behavior and internal dynamics.

1.1. The Poisson-Nernst-Planck model

The Poisson-Nernst-Planck (PNP) system serves as the foundational continuum model for ionic flows. It can be derived from multiple theoretical frameworks, including molecular dynamics [44], Boltzmann equations [3], and variational principles [26–28]. The classical Poisson-Nernst-Planck (cPNP) system, the simplest form of the PNP model, incorporates only the ideal electrochemical potential $\mu_k^{id}(x)$ from (1.6), treating ions as point charges. This model has been extensively simulated and analyzed for a wide range of applications (see, [1,3–5,10,20,24,35,42,45,46,49, 53,54]).

The narrow cross-sections of ion channels compared to their lengths allows for a reduction of the three-dimensional PNP system to a quasi-one-dimensional model, an approach first proposed in [42] and later rigorously justified in [37] for special cases. For $k = 1, 2, \ldots, n$, a quasi-one-dimensional steady-state PNP model takes the form:

$$\begin{aligned} &\frac{1}{h(x)}\frac{d}{dx}\Big(\varepsilon_r(x)\varepsilon_0 h(x)\frac{d\Phi}{dx}\Big) = -e\Big(\sum_{s=1}^{n} z_s c_s + Q(x)\Big), \\ &\frac{d\mathcal{J}_k}{dx} = 0, \quad -\mathcal{J}_k = \frac{1}{k_B T} D_k(x) h(x) c_k \frac{d\mu_k}{dx}, \end{aligned} \tag{1.1}$$

where $x \in [0,1]$ is the coordinate along the axis of the channel that is normalized to $[0,1]$, $h(x)$ is the area of cross-section of the channel over the location x, $Q(x)$ is the permanent charge density, $\varepsilon_r(x)$ is the relative dielectric coefficient, ε_0 is the vacuum permittivity, e is the elementary charge, k_B is the Boltzmann constant, T is the absolute temperature, Φ is the electric potential. For the kth ion species, c_k is the concentration, z_k is the valence, μ_k is the electrochemical potential depending on Φ and c_k, $\mathcal{J}_k(x)$ is the flux density through the cross-section over x, and $D_k(x)$ is the diffusion coefficient.

For $k = 1, 2, \cdots, n$, system (1.1) is governed by the boundary conditions given below (see [14] for a derivation):

$$\Phi(0) = \mathcal{V}, \quad c_k(0) = L_k > 0; \quad \Phi(1) = 0, \quad c_k(1) = R_k > 0. \tag{1.2}$$

Beyond the effects of boundary conditions and ion properties, the distribution of permanent charge serves as the principal determinant of channel type [18], providing a crucial component to the complex behaviors in ion channels. Specifically, the permanent charge reflects the protein structure and is influenced by factors such as atomic positions and channel geometry [15]. The permanent charge $Q(x)$ is typically modeled as a piecewise constant function. Specifically, we partition the interval $[0,l]$ as $x_0 = 0 < x_1 < \cdots < x_{m-1} < x_m = l$ and define $Q(x) = Q_j$ for $x \in (x_{j-1}, x_j)$, where each Q_j is a constant. The conditions $Q_1 = Q_m = 0$ are imposed, with the intervals $[x_0, x_1]$ and $[x_{m-1}, x_m]$ interpreted as the reservoirs without permanent charges.

Within the framework of geometric singular perturbation theory, the work in [14] established the local existence and uniqueness of solutions to the boundary value problem (1.1)-(1.2) with

one cation and one anion. The permanent charge $Q(x)$ was modeled by

$$Q(x) = 0 \text{ if } 0 < x < a; \quad Q(x) = Q_0 \text{ if } a < x < b; \quad Q(x) = 0 \text{ if } b < x < 1. \tag{1.3}$$

Building on this, [31] investigated the case of small Q_0 in (1.3), employing a regular perturbation analysis to examine its effects on ionic flows. This study revealed interesting flow properties and emphasized the critical role of permanent charge in shaping these properties.

Macroscopic reservoirs are essential for modeling channels or transistors [9, 19–21], but their boundary conditions introduce boundary layers that can significantly influence the device's core region, with charge layers having long-range effects. Nonetheless, studies of key ionic flow properties (individual fluxes and I-V relations for permeation and selectivity) commonly simplify this by imposing electroneutrality boundary conditions (see, [1, 6, 7, 30–33, 36, 53]), defined as follows:

$$\sum_{s=1}^{n} z_s L_s = \sum_{s=1}^{n} z_s R_s = 0. \tag{1.4}$$

Although the electroneutrality condition (1.4) significantly simplifies the analysis of ionic flow dynamics, it also precludes the examination of boundary layer effects, which carry critical physical information.

Within the framework of ion channel biophysics, the boundary layer typically refers to the narrow region near the channel entrance or exit. In this region, local electroneutrality is often violated, leading to sharp variations in ion concentration and electrical potential, which in turn play a decisive role in the overall ion transport behavior. Boundary layer effects exert a fundamental influence on key macroscopic functional properties, including ion selectivity, the nonlinear current–voltage relations, and voltage-dependent rectification behavior. Consequently, neglecting the boundary layer would impede a precise comprehension of the fundamental mechanisms driving these phenomena.

A complete understanding of ionic flow mechanisms through membrane channels requires careful consideration of boundary layer effects. Given this sensitivity of electric potentials to these layers, our study employs the PNP model under the assumption of partial neutral boundary condition, which is defined as follows:

$$-z_2 L_2 = \sigma(z_1 L_1) \text{ and } -z_2 R_2 = z_1 R_1, \tag{1.5}$$

where σ is some positive constant not equal to 1 ($\sigma = 1$ in (1.5) implies neutral state).

In this work, our analysis reveals richer qualitative properties of ionic flows beyond those observable under electroneutrality conditions. Furthermore, we examines boundary layer effects on ionic flows through a one-dimensional classical PNP model with small permanent charges. A primary objective is to characterize the nonlinear interplay among key parameters, including channel geometry, permanent charge, boundary conditions, and boundary layers. These results offer a mechanism for controlling ionic flows through the application of boundary electric potentials.

1.2. The boundary value problem and settings

Under the assumption of partial neutral boundary condition (1.5), we take the following settings:

(i). Two ion species ($n = 2$) with $z_1 > 0$ and $z_2 < 0$.

(ii). The permanent charge $Q(x)$ is modeled by (1.3).

(iii). The model only includes the ideal component of the electrochemical potential, which is defined as

$$\mu_k^{id}(x) = z_k e\Phi(x) + k_B T \ln \frac{c_k(x)}{c_0}, \tag{1.6}$$

where c_0 is some characteristic number density.

(iv). $\varepsilon_r(x) = \varepsilon_r$ and $D_k(x) = D_k$.

Under the assumptions (i)–(iv), we first make the following dimensionless rescaling. Let

$$\phi = \frac{e}{k_B T}\Phi, \quad V = \frac{e}{k_B T}\mathcal{V}, \quad \varepsilon^2 = \frac{\varepsilon_r \varepsilon_0 k_B T}{e^2}, \quad J_k = \frac{\mathcal{J}_k}{D_k}.$$

Correspondingly, for $k = 1, 2$, the boundary value problem (1.1)-(1.2) becomes

$$\begin{aligned} &\frac{\varepsilon^2}{h(x)}\frac{d}{dx}\left(h(x)\frac{d}{dx}\phi\right) = -z_1 c_1 - z_2 c_2 - Q(x), \\ &h(x)\frac{dc_k}{dx} + z_k h(x) c_k \frac{d\phi}{dx} = -J_k, \quad \frac{dJ_k}{dx} = 0, \end{aligned} \tag{1.7}$$

with the boundary conditions

$$\phi(0) = V,\ c_k(0) = L_k; \quad \phi(1) = 0,\ c_k(1) = R_k. \tag{1.8}$$

1.3. Motivation and the main results

This work focuses on elucidating the mechanism by which boundary layers influence ionic flows in the PNP system (1.7)-(1.8) with small permanent charges. By considering the case of small $|Q_0|$ relative to the boundary concentrations L_k and R_k, the authors in [31] subsequently derive Q_0-expanded approximations for the individual fluxes:

$$J_k = J_{k0} + J_{k1} Q_0 + o(Q_0), \quad k = 1, 2, \tag{1.9}$$

where

$$\begin{aligned} J_{10} =& \frac{(c_1^L - c_1^R)(z_1 V + \ln L_1 - \ln R_1)}{H(1)(\ln c_1^L - \ln c_1^R)},\ J_{20} = \frac{(c_2^L - c_2^R)(z_2 V + \ln L_2 - \ln R_2)}{H(1)(\ln c_2^L - \ln c_2^R)}, \\ J_{11} =& \frac{A(z_2(1-B)\lambda + 1)}{(z_1 - z_2)H(1)}(z_1\lambda + 1),\ J_{21} = \frac{A(z_1(1-B)\lambda + 1)}{(z_2 - z_1)H(1)}(z_2\lambda + 1), \end{aligned} \tag{1.10}$$

with

$$\begin{aligned} &\lambda = \frac{\phi^L - \phi^R}{\ln c_1^L - \ln c_1^R}, \quad A = \frac{(c_1^L - c_1^R)(c_{10}^b - c_{10}^a)}{c_{10}^a c_{10}^b (\ln c_1^L - \ln c_1^R)}, \quad B = \frac{\ln c_{10}^b - \ln c_{10}^a}{A}, \\ &\phi^L = V - \frac{1}{z_1 - z_2}\ln\frac{-z_2 L_2}{z_1 L_1}, \quad z_1 c_1^L = -z_2 c_2^L = (z_1 L_1)^{\frac{-z_2}{z_1 - z_2}}(-z_2 L_2)^{\frac{z_1}{z_1 - z_2}}, \\ &\phi^R = -\frac{1}{z_1 - z_2}\ln\frac{-z_2 R_2}{z_1 L_1}, \quad z_1 c_1^R = -z_2 c_2^R = (z_1 R_1)^{\frac{-z_2}{z_1 - z_2}}(-z_2 R_2)^{\frac{z_1}{z_1 - z_2}}, \\ &c_{10}^a = c_1^L + \alpha(c_1^R - c_1^L), \quad c_{10}^b = c_1^L + \beta(c_1^R - c_1^L), \end{aligned}$$

$$\alpha = \frac{H(a)}{H(1)}, \quad \beta = \frac{H(b)}{H(1)}, \quad H(x) = \int_0^x \frac{1}{h(s)} ds.$$

Here, V denotes the voltage. c_k^L and c_k^R represent the concentrations of the k-th ion species at the leftmost and rightmost ends of the channel, respectively.

While previous research [50] has established the influence of small permanent charges on ion fluxes by examining the signs of $J_{k0}J_{k1}$, it does not account for the critical role of J_{k1} itself. In this work, we address this by providing a detailed analysis of J_{k1}, the leading-order term in the individual fluxes that captures the effects of small permanent charges and channel geometry. In particular, the condition $J_{k0} = 0$ corresponds to a unique critical potential, denoted V_{kc}^1, while the condition $J_{k1} = 0$ is associated with two distinct critical potentials, V_{kc}^1 and V_{kc}^2 (see Lemma 2.1 and Theorem 2.1). By employing more generalized boundary conditions, we first investigate the qualitative properties of both J_{k0} and J_{k1} through their signs. Furthermore, we compare the critical potentials V_{kc}^1 and V_{kc}^2 under certain conditions, thereby offering a more comprehensive understanding of how permanent charge governs individual fluxes within different potential intervals.

The remainder of this paper is structured as follows. Section 2 provides a detailed analysis of how boundary layers and small permanent charges affect individual fluxes. In Section 3, numerical simulations offer visual validation of our analytical findings. Finally, the conclusions of this work are presented in Section 4.

2. Influence of permanent charges on individual fluxes with partial boundary layers

Under assumption (1.5), we analyze the influence of permanent charges and channel geometry on the individual fluxes. Let $t = \frac{L_1}{R_1}$ and $\sigma_1 = \sigma^{\frac{z_1}{z_1 - z_2}}$, equation (1.10) can be expressed as

$$\begin{aligned}
J_{10} =& \frac{R_1(\sigma_1 t - 1)(z_1 V + \ln t)}{\ln(\sigma_1 t) H(1)}, \quad J_{20} = -\frac{z_1}{z_2} \frac{R_1(\sigma_1 t - 1)(z_2 V + \ln(\sigma t))}{\ln(\sigma_1 t) H(1)}, \\
J_{11} =& \frac{A_1 \big(z_2 A_2 V + (1 + \frac{z_2}{z_1 - z_2}(1 - A_2)) \ln \sigma + \ln t\big)\big(z_1 V + \ln t\big)}{(z_1 - z_2) \ln^2(\sigma_1 t) H(1)}, \\
J_{21} =& \frac{A_1 \big(z_1 A_2 V + \frac{z_1}{z_1 - z_2}(1 - A_2) \ln \sigma + \ln t\big)\big(z_2 V + \ln(\sigma t)\big)}{(z_2 - z_1) \ln^2(\sigma_1 t) H(1)},
\end{aligned} \tag{2.1}$$

where

$$A_1 = -\frac{(\beta - \alpha)(\sigma_1 t - 1)^2}{\omega(\alpha)\omega(\beta) \ln(\sigma_1 t)}, \quad A_2 = \frac{s(\beta)}{(\beta - \alpha)(\sigma_1 t - 1)^2},$$

with

$$\begin{aligned}
&s(\beta) = \omega(\alpha)\omega(\beta) \ln(\sigma_1 t) \ln \frac{\omega(\beta)}{\omega(\alpha)} + (\beta - \alpha)(\sigma_1 t - 1)^2, \\
&\omega(\alpha) = (1 - \alpha)\sigma_1 t + \alpha > 0, \quad \omega(\beta) = (1 - \beta)\sigma_1 t + \beta > 0.
\end{aligned} \tag{2.2}$$

Note here that we introduce a new parameter σ_1, which is defined based on parameter σ in the boundary conditions (1.5) to quantify the influence of the boundary layer on the ion flux.

In this work, we restrict our discussion to the case $A_2 \neq 0$. When $\sigma = 1$, the expression for J_{k1} in (2.1) reduces to the electroneutral case previously established in [31].

Notice that V_{1c}^1, V_{1c}^2 are two roots of $J_{11}(V) = 0$, and V_{2c}^1, V_{2c}^2 are two roots of $J_{21}(V) = 0$, respectively, which are given by

$$\begin{aligned} V_{1c}^1 &= -\frac{\ln t}{z_1}, \quad V_{1c}^2 = \frac{1}{z_1 - z_2}\Big(\ln\sigma - \frac{z_1 \ln\sigma + (z_1 - z_2)\ln t}{z_2 A_2}\Big), \\ V_{2c}^1 &= -\frac{\ln \sigma t}{z_2}, \quad V_{2c}^2 = \frac{1}{z_1 - z_2}\Big(\ln\sigma - \frac{z_1 \ln\sigma + (z_1 - z_2)\ln t}{z_1 A_2}\Big). \end{aligned} \tag{2.3}$$

For $k = 1, 2$, we observe that J_{k0} and J_{k1} share a common zero, specifically at the potential V_{kc}^1. Based on the equations (2.1), the following conclusion regarding J_{k0} can be immediately established.

Lemma 2.1. *For the monotonicity of $J_{k0}(V)$, one has*

(i) *J_{10} is monotonically increasing in V. Furthermore, $J_{10} < 0$ for $V \in (-\infty, V_{1c}^1)$ and $J_{10} > 0$ for $V \in (V_{1c}^1, +\infty)$.*

(ii) *J_{20} is monotonically decreasing in V. Furthermore, $J_{20} > 0$ for $V \in (-\infty, V_{2c}^1)$ and $J_{20} < 0$ for $V \in (V_{2c}^1, +\infty)$.*

We firstly define the following functions, which will be used frequently in our analysis. For $t > 0$ and $\sigma_1 t \neq 1$, we set

$$\begin{aligned} \gamma_1(t) &= \frac{\sigma_1 t}{\sigma_1 t - 1} - \frac{1}{\ln(\sigma_1 t)}, \\ \gamma_2(t) &= \frac{\sigma_1 t}{\sigma_1 t - 1} - \Big(1 - \frac{z_1}{z_2}\Big)\frac{1}{\ln(\sigma_1 t)}, \\ \gamma_3(t) &= \frac{\sigma_1 t}{\sigma_1 t - 1} - \Big(1 - \frac{z_2}{z_1}\Big)\frac{1}{\ln(\sigma_1 t)}. \end{aligned} \tag{2.4}$$

2.1. An analysis of the fluxes J_{k1}

For $k = 1, 2$, J_{k1} is the dominant term characterizing the influence of permanent charges on individual ionic fluxes. The properties of J_{k1} are analyzed in this subsection.

Our analysis begins with an examination of the sign of the V^2 coefficient in J_{k1} for $k = 1, 2$, as it is crucial for the subsequent discussion. Direct calculation on equations (2.1) lead to

$$\frac{d^2 J_{11}}{dV^2} = -\frac{d^2 J_{21}}{dV^2} = \frac{z_1 z_2 A_1 A_2}{(z_1 - z_2)\ln^2(\sigma_1 t) H(1)}.$$

The sign of A_1 can be readily established.

Lemma 2.2. *A_1 and $\sigma_1 t - 1$ have opposite signs.*

We next consider the sign of A_2, which will be used later for our analysis.

Lemma 2.3. *Assume $t = \frac{L_1}{R_1}$, $\gamma_1(t)$ is defined by (2.4) and*

$$s_1(\alpha) = (1 - \alpha)(1 - \sigma_1 t)^2 - \omega(\alpha)\ln(\sigma_1 t)\ln\omega(\alpha).$$

Then,

(i) *For* $\sigma_1 t > 1$,

(i1) *When* $\alpha \geq \gamma_1(t)$, $A_2 > 0$;

(i2) *When* $\alpha < \gamma_1(t)$, $A_2(\beta)$ *has a unique zero* $\beta_1 \in (\alpha, 1)$, *with* $A_2 < 0$ *for* $\beta \in (\alpha, \beta_1)$ *and* $A_2 > 0$ *for* $\beta \in (\beta_1, 1)$.

(ii) *For* $\sigma_1 t < 1$,

(ii1) *For* $\alpha \geq \gamma_1(t)$, *one has* $A_2 < 0$;

(ii2) *For* $\alpha < \gamma_1(t)$, $s_1(\alpha)$ *has a unique zero* $\alpha_1 \in (0, 1)$, *such that*

(ii21) *When* $\alpha < \gamma_1(t) \leq \alpha_1$ *or* $\alpha < \alpha_1 < \gamma_1(t)$, $A_2 > 0$;

(ii22) *When* $\alpha_1 < \alpha < \gamma_1(t)$, $A_2(\beta)$ *has a unique zero* $\beta_2 \in (\alpha, 1)$, *with* $A_2 > 0$ *for* $\beta \in (\alpha, \beta_2)$ *and* $A_2 < 0$ *for* $\beta \in (\beta_2, 1)$.

Proof. We will proceed to prove statement (i), as the remaining statements can be established by an similar argument. Obviously, A_2 has the same sign as that of $s(\beta)$. Direct calculation on $s(\beta)$ leads to

$$s'(\beta) = \left(\omega(\alpha)\ln\frac{\omega(\beta)}{\omega(\alpha)} + (1-\sigma_1 t)(\alpha - \gamma_1(t))\right)(1-\sigma_1 t)\ln(\sigma_1 t),$$
$$s''(\beta) = \frac{\omega(\alpha)}{\omega(\beta)}(1-\sigma_1 t)^2\ln(\sigma_1 t),$$

where $\gamma_1(t)$ is defined in (2.4). When $\sigma_1 t > 1$, we have $s''(\beta) > 0$, which implies $s(\beta)$ is concave upward. If $\beta \to \alpha$, then

$$\lim_{\beta\to\alpha} s(\beta) = 0, \quad \lim_{\beta\to\alpha} s'(\beta) = (1-\sigma_1 t)^2(\alpha - \gamma_1(t))\ln(\sigma_1 t).$$

Under the condition $\alpha \geq \gamma_1(t)$, we have $\lim\limits_{\beta\to\alpha} s'(\beta) \geq 0$. Together with $s''(\beta) > 0$, we conclude that $s(\beta) > 0$.

We now turn to the case $\alpha < \gamma_1(t)$, where $\lim\limits_{\beta\to\alpha} s'(\beta) < 0$. Our objective is to establish the sign of $s(1)$, as this is key to characterizing the sign of $s(\beta)$ over the entire interval. Let

$$s_1(\alpha) = s(1) = (1-\alpha)(1-\sigma_1 t)^2 - \omega(\alpha)\ln(\sigma_1 t)\ln\omega(\alpha).$$

By calculation, one has

$$s_1'(\alpha) = -(1-\sigma_1 t)\big((1-\sigma_1 t) + (1+\ln\omega(\alpha))\ln(\sigma_1 t)\big),$$
$$s_1''(\alpha) = -\frac{1}{\omega(\alpha)}(1-\sigma_1 t)^2\ln(\sigma_1 t) < 0.$$

Clearly, $s_1(1) = 0$. Set

$$s_{11}(t^*) = s_1(0) = (1-t^*)^2 - t^*\ln^2 t^*,$$

where $t^* = \sigma_1 t > 1$. Direct calculation on $s_{11}(t^*)$ yields

$$s_{11}'(t^*) = 2(t^*-1) - \ln^2 t^* - 2\ln t^*, \quad s_{11}''(t^*) = \frac{2}{t^*}(t^* - 1 - \ln t^*) > 0.$$

It's easy to check that $s_{11}(1) = s_{11}'(1) = 0$, and thus $s_{11}(t^*) = s_1(0) > 0$, which indicates that $s_1(\alpha) = s(1) > 0$. Note that $s''(\beta) > 0$. Therefore, there exists a unique $\beta_1 \in (\alpha, 1)$ such that $s(\beta) < 0$ for $\beta \in (\alpha, \beta_1)$ and $s(\beta) > 0$ for $\beta \in (\beta_1, 1)$. It completes the proof. □

It follows directly from Lemmas 2.2 and 2.3 that

Theorem 2.1. *Assume $t = \frac{L_1}{R_1}$ and $\gamma_1(t)$ is defined by (2.4). Let $V_{min} = \min\{V_{kc}^1, V_{kc}^2\}$ and $V_{max} = \max\{V_{kc}^1, V_{kc}^2\}$, then*

(i) *$\frac{d^2J_{11}}{dV^2} > 0$ and $\frac{d^2J_{21}}{dV^2} < 0$ if one of the following conditions holds:*

(i1) *$\alpha \geq \gamma_1(t)$;*

(i2) *$\sigma_1 t > 1$, $\alpha < \gamma_1(t)$ and $\beta \in (\beta_1, 1)$;*

(i3) *$\sigma_1 t < 1$, $\alpha_1 < \alpha < \gamma_1(t)$ and $\beta \in (\beta_2, 1)$.*

Moreover, the signs of J_{11} and J_{21} are as follows:

(a) *For $V \in (V_{min}, V_{max})$, $J_{11} < 0$ and $J_{21} > 0$, that is, (small) positive permanent charge reduces J_1 but enhances J_2.*

(b) *For $V \in (-\infty, V_{min})$ or $V \in (V_{max}, +\infty)$, $J_{11} > 0$ and $J_{21} < 0$, that is, (small) positive permanent charge enhances J_1 but reduces J_2.*

(ii) *$\frac{d^2J_{11}}{dV^2} < 0$ and $\frac{d^2J_{21}}{dV^2} > 0$ if one of the following conditions holds:*

(ii1) *$\sigma_1 t > 1$, $\alpha < \gamma_1(t)$ and $\beta \in (\alpha, \beta_1)$;*

(ii2) *$\sigma_1 t < 1$ and $\alpha < \min\{\alpha_1, \gamma_1(t)\}$;*

(ii3) *$\sigma_1 t < 1$, $\alpha_1 < \alpha < \gamma_1(t)$ and $\beta \in (\alpha, \beta_2)$.*

Moreover, the signs of J_{11} and J_{21} are as follows:

(a) *For $V \in (V_{min}, V_{max})$, $J_{11} > 0$ and $J_{21} < 0$, that is, (small) positive permanent charge enhances J_1 but reduces J_2.*

(b) *For $V \in (-\infty, V_{min})$ or $V \in (V_{max}, +\infty)$, $J_{11} < 0$ and $J_{21} > 0$, that is, (small) positive permanent charge reduces J_1 but enhances J_2.*

In the following, we present a rigorous analytical computation to compare the magnitudes of V_{kc}^1 and V_{kc}^2 for $k = 1, 2$. It follows from (2.3) that

$$V_{1c}^2 - V_{1c}^1 = \frac{\ln(\sigma_1 t) f_1(\beta)}{z_1 z_2 s(\beta)}, \quad V_{2c}^2 - V_{2c}^1 = \frac{\ln(\sigma_1 t) f_2(\beta)}{z_1 z_2 s(\beta)}.$$

To facilitate the subsequent analysis, we first introduce the following two functions.

$$f_1(\beta) = z_2\omega(\alpha)\omega(\beta)\ln(\sigma_1 t)\ln\frac{\omega(\beta)}{\omega(\alpha)} + (z_2 - z_1)(\beta - \alpha)(\sigma_1 t - 1)^2,$$

$$f_2(\beta) = z_1\omega(\alpha)\omega(\beta)\ln(\sigma_1 t)\ln\frac{\omega(\beta)}{\omega(\alpha)} + (z_1 - z_2)(\beta - \alpha)(\sigma_1 t - 1)^2.$$

Then, it follows

Lemma 2.4. *Assume $t = \frac{L_1}{R_1}$, $\gamma_2(t)$ is defined by (2.4) and*

$$p_1(t) = (z_2 - z_1)(1 - t)^2 - z_2 t \ln^2 t,$$
$$f_{11}(\alpha) = (z_2 - z_1)(1 - \alpha)(1 - \sigma_1 t)^2 - z_2\omega(\alpha)\ln(\sigma_1 t)\ln\omega(\alpha).$$

Then,

(i) *For $\sigma_1 t > 1$,*

(i1) *When $\alpha \geq \gamma_2(t)$, $f_1(\beta) < 0$;*

(i2) *When* $\alpha < \gamma_2(t)$, $f_1(\beta)$ *has a unique zero* $\beta_3 \in (\alpha, 1)$, *with* $f_1(\beta) > 0$ *for* $\beta \in (\alpha, \beta_3)$ *and* $f_1(\beta) < 0$ *for* $\beta \in (\beta_3, 1)$.

(ii) *For* $\sigma_1 t < 1$, *when* $\alpha \geq \gamma_2(t)$, $f_1(\beta) > 0$; *when* $\alpha < \gamma_2(t)$, $p_1(t)$ *has a unique zero* $t_1 \in (0, 1)$, *such that*

(ii1) *For* $\sigma_1 t \in (t_1, 1)$, *one has* $f_1(\beta) < 0$;

(ii2) *For* $\sigma_1 t \in (0, t_1)$, $f_{11}(\alpha)$ *has a unique zero* $\alpha_2 \in (0, 1)$, *such that*

(ii21) *When* $\alpha < \gamma_2(t) \leq \alpha_2$ *or* $\alpha < \alpha_2 < \gamma_2(t)$, $f_1(\beta) < 0$;

(ii22) *When* $\alpha_2 < \alpha < \gamma_2(t)$, $f_1(\beta)$ *has a unique zero* $\beta_4 \in (\alpha, 1)$, *with* $f_1(\beta) < 0$ *for* $\beta \in (\alpha, \beta_4)$ *and* $f_1(\beta) > 0$ *for* $\beta \in (\beta_4, 1)$.

Proof. Statement (i) is proved below, with the rest following from similar reasoning. Direct calculation on $f_1(\beta)$ leads to

$$f_1'(\beta) = z_2\left(\omega(\alpha)\ln\frac{\omega(\beta)}{\omega(\alpha)} + (1-\sigma_1 t)(\alpha - \gamma_2(t))\right)(1-\sigma_1 t)\ln(\sigma_1 t),$$
$$f_1''(\beta) = z_2\frac{\omega(\alpha)}{\omega(\beta)}(1-\sigma_1 t)^2\ln(\sigma_1 t) < 0,$$

where $\gamma_2(t)$ is defined in (2.4) and $\sigma_1 t > 1$. As $\beta \to \alpha$, it holds that

$$\lim_{\beta\to\alpha} f_1(\beta) = 0, \quad \lim_{\beta\to\alpha} f_1'(\beta) = z_2(1-\sigma_1 t)^2(\alpha - \gamma_2(t))\ln(\sigma_1 t).$$

Given $\alpha \geq \gamma_2(t)$, we observe that $\lim\limits_{\beta\to\alpha} f_1'(\beta) \leq 0$ and $f_1''(\beta) < 0$, and thus $f_1(\beta) < 0$.

For the case $\alpha < \gamma_2(t)$, characterized by $\lim\limits_{\beta\to\alpha} f_1'(\beta) > 0$, and we proceed to determine the sign of $f_1(1)$. Define

$$f_{11}(\alpha) = f_1(1) = (z_2 - z_1)(1-\alpha)(1-\sigma_1 t)^2 - z_2\omega(\alpha)\ln(\sigma_1 t)\ln\omega(\alpha).$$

Therefore,

$$f_{11}'(\alpha) = (z_1 - z_2)(1-\sigma_1 t)^2 - z_2(1-\sigma_1 t)(1+\ln\omega(\alpha))\ln(\sigma_1 t),$$
$$f_{11}''(\alpha) = -\frac{z_2}{\omega(\alpha)}(1-\sigma_1 t)^2\ln(\sigma_1 t) > 0.$$

Since one can easily verify that $f_{11}(0) < 0$ and $f_{11}(1) = 0$, it follows that $f_{11}(\alpha) = f_1(1) < 0$. Therefore, there exists a unique $\beta_3 \in (\alpha, 1)$ such that $f_1(\beta) > 0$ for $\beta \in (\alpha, \beta_3)$ and $f_1(\beta) < 0$ for $\beta \in (\beta_3, 1)$. It completes the proof. □

Since the proof follows an argument similar to that of Lemma 2.4, we omit the details and state the conclusion directly as follows.

Lemma 2.5. *Assume* $t = \frac{L_1}{R_1}$, $\gamma_3(t)$ *is defined by (2.4) and*

$$p_2(t) = (z_1 - z_2)(1-t)^2 - z_1 t\ln^2 t,$$
$$f_{21}(\alpha) = (z_1 - z_2)(1-\alpha)(1-\sigma_1 t)^2 - z_1\omega(\alpha)\ln(\sigma_1 t)\ln\omega(\alpha).$$

Then,

(i) *For* $\sigma_1 t > 1$,

(i1) *When* $\alpha \geq \gamma_3(t)$, $f_2(\beta) > 0$;

(i2) *When* $\alpha < \gamma_3(t)$, $f_2(\beta)$ *has a unique zero* $\beta_5 \in (\alpha, 1)$, *with* $f_2(\beta) < 0$ *for* $\beta \in (\alpha, \beta_5)$ *and* $f_2(\beta) > 0$ *for* $\beta \in (\beta_5, 1)$.

(ii) *For* $\sigma_1 t < 1$, *when* $\alpha \geq \gamma_3(t)$, $f_2(\beta) < 0$; *when* $\alpha < \gamma_3(t)$, $p_2(t)$ *has a unique zero* $t_2 \in (0, 1)$, *such that*

(ii1) *For* $\sigma_1 t \in (t_2, 1)$, *one has* $f_2(\beta) > 0$;

(ii2) *For* $\sigma_1 t \in (0, t_2)$, $f_{21}(\alpha)$ *has a unique zero* $\alpha_3 \in (0, 1)$, *such that*

(ii21) *When* $\alpha < \gamma_3(t) \leq \alpha_3$ *or* $\alpha < \alpha_3 < \gamma_3(t)$, $f_2(\beta) > 0$;

(ii22) *When* $\alpha_3 < \alpha < \gamma_3(t)$, $f_2(\beta)$ *has a unique zero* $\beta_6 \in (\alpha, 1)$, *with* $f_2(\beta) > 0$ *for* $\beta \in (\alpha, \beta_6)$ *and* $f_2(\beta) < 0$ *for* $\beta \in (\beta_6, 1)$.

Combined with Lemmas 2.3 and 2.4, we obtain the following result.

Theorem 2.2. *Assume* $t = \frac{L_1}{R_1}$. *One has*

(i) $V_{1c}^2 > V_{1c}^1$ *under one of the following conditions:*

(i1) $\sigma_1 t > 1$,

(1) $\alpha \geq \gamma_1(t)$;

(2) $\gamma_2(t) \leq \alpha < \gamma_1(t)$ *and* $\beta \in (\beta_1, 1)$;

(3) $\alpha < \gamma_2(t)$ *and* $\beta \in (\alpha, \min\{\beta_1, \beta_3\}) \cup (\max\{\beta_1, \beta_3\}, 1)$;

(i2) $\sigma_1 t < 1$,

(1) $\alpha_1 < \alpha < \min\{\alpha_2, \gamma_1(t)\}$ *and* $\beta \in (\beta_2, 1)$;

(2) $\alpha_2 < \alpha < \alpha_1 < \gamma_1(t)$ *and* $\beta \in (\beta_4, 1)$;

(3) $\max\{\alpha_1, \alpha_2\} < \alpha < \gamma_1(t)$ *and* $\beta \in (\min\{\beta_2, \beta_4\}, \max\{\beta_2, \beta_4\})$;

(4) $t_1 < \sigma_1 t$, $\gamma_1(t) \leq \alpha < \gamma_2(t)$ *or* $\alpha_1 < \alpha < \gamma_1(t)$ *and* $\beta \in (\beta_2, 1)$;

(i3) $\sigma_1 t < t_1 < 1$,

(1) $\gamma_1(t) \leq \alpha < \min\{\alpha_2, \gamma_2(t)\}$;

(2) $\max\{\alpha_2, \gamma_1(t)\} < \alpha < \gamma_2(t)$ *and* $\beta \in (\alpha, \beta_4)$;

(3) $\alpha_2 \geq \gamma_2(t)$, $\alpha_1 < \alpha < \gamma_1(t)$ *and* $\beta \in (\beta_2, 1)$;

(4) $\alpha_2 < \gamma_2(t)$, $\alpha_2 < \alpha < \gamma_1(t) \leq \alpha_1$ *and* $\beta \in (\beta_4, 1)$.

(ii) $V_{1c}^2 < V_{1c}^1$ *under one of the following conditions:*

(ii1) $\sigma_1 t > 1$,

(1) $\gamma_2(t) \leq \alpha < \gamma_1(t)$ *and* $\beta \in (\alpha, \beta_1)$;

(2) $\alpha < \gamma_2(t)$ *and* $\beta \in (\min\{\beta_1, \beta_3\}, \max\{\beta_1, \beta_3\})$;

(ii2) $\sigma_1 t < 1$,

(1) $\alpha \geq \gamma_2(t)$;

(2) $\alpha < \min\{\alpha_1, \alpha_2\}$, $\alpha_1 < \gamma_1(t)$ *and* $\alpha_2 < \gamma_2(t)$;

(3) $\alpha_1 < \alpha < \min\{\alpha_2, \gamma_1(t)\}$ *and* $\beta \in (\alpha, \beta_2)$;

(4) $\alpha_2 < \alpha < \alpha_1 < \gamma_1(t)$ *and* $\beta \in (\alpha, \beta_4)$;

(5) $\max\{\alpha_1, \alpha_2\} < \alpha < \gamma_1(t)$ *and* $\beta \in (\alpha, \min\{\beta_2, \beta_4\}) \cup (\max\{\beta_2, \beta_4\}, 1)$;

(6) $t_1 < \sigma_1 t$, $\alpha < \min\{\alpha_1, \gamma_1(t)\}$ *or* $\alpha_1 < \alpha < \gamma_1(t)$ *and* $\beta \in (\alpha, \beta_2)$;

(ii3) $\sigma_1 t < t_1 < 1$,

(1) $\max\{\alpha_2, \gamma_1(t)\} < \alpha < \gamma_2(t)$ *and* $\beta \in (\beta_4, 1)$;
(2) $\alpha_2 \geq \gamma_2(t)$ *and* $\alpha < \min\{\alpha_1, \gamma_1(t)\}$;
(3) $\alpha_2 \geq \gamma_2(t)$, $\alpha_1 < \alpha < \gamma_1(t)$ *and* $\beta \in (\alpha, \beta_2)$;
(4) $\alpha < \min\{\alpha_2, \gamma_1(t)\}$, $\alpha_1 \geq \gamma_1(t)$ *and* $\alpha_2 < \gamma_2(t)$;
(5) $\alpha_2 < \gamma_2(t)$, $\alpha_2 < \alpha < \gamma_1(t) \leq \alpha_1$ *and* $\beta \in (\alpha, \beta_4)$.

Based on Lemmas 2.3 and 2.5, the order of V_{2c}^1 and V_{2c}^2 can easily be established, yielding the conclusion as follows.

Theorem 2.3. *Assume* $t = \frac{L_1}{R_1}$. *One has*

(i) $V_{2c}^2 < V_{2c}^1$ *under one of the following conditions:*
(i1) $\sigma_1 t > 1$,
(1) $\alpha \geq \gamma_1(t)$;
(2) $\gamma_3(t) \leq \alpha < \gamma_1(t)$ *and* $\beta \in (\beta_1, 1)$;
(3) $\alpha < \gamma_3(t)$ *and* $\beta \in (\alpha, \min\{\beta_1, \beta_5\}) \cup (\max\{\beta_1, \beta_5\}, 1)$;
(i2) $\sigma_1 t < 1$,
(1) $\alpha_1 < \alpha < \min\{\alpha_3, \gamma_1(t)\}$ *and* $\beta \in (\beta_2, 1)$;
(2) $\alpha_3 < \alpha < \alpha_1 < \gamma_1(t)$ *and* $\beta \in (\beta_6, 1)$;
(3) $\max\{\alpha_1, \alpha_3\} < \alpha < \gamma_1(t)$ *and* $\beta \in (\min\{\beta_2, \beta_6\}, \max\{\beta_2, \beta_6\})$;
(4) $t_2 < \sigma_1 t$, $\gamma_1(t) \leq \alpha < \gamma_3(t)$ *or* $\alpha_1 < \alpha < \gamma_1(t)$ *and* $\beta \in (\beta_2, 1)$;
(i3) $\sigma_1 t < t_2 < 1$,
(1) $\gamma_1(t) \leq \alpha < \min\{\alpha_3, \gamma_3(t)\}$;
(2) $\max\{\alpha_3, \gamma_1(t)\} < \alpha < \gamma_3(t)$ *and* $\beta \in (\alpha, \beta_6)$;
(3) $\alpha_3 \geq \gamma_3(t)$, $\alpha_1 < \alpha < \gamma_1(t)$ *and* $\beta \in (\beta_2, 1)$;
(4) $\alpha_3 < \gamma_3(t)$, $\alpha_3 < \alpha < \gamma_1(t) \leq \alpha_1$ *and* $\beta \in (\beta_6, 1)$.

(ii) $V_{2c}^2 > V_{2c}^1$ *under one of the following conditions:*
(ii1) $\sigma_1 t > 1$,
(1) $\gamma_3(t) \leq \alpha < \gamma_1(t)$ *and* $\beta \in (\alpha, \beta_1)$;
(2) $\alpha < \gamma_3(t)$ *and* $\beta \in (\min\{\beta_1, \beta_5\}, \max\{\beta_1, \beta_5\})$;
(ii2) $\sigma_1 t < 1$,
(1) $\alpha \geq \gamma_3(t)$;
(2) $\alpha < \min\{\alpha_1, \alpha_3\}$, $\alpha_1 < \gamma_1(t)$ *and* $\alpha_3 < \gamma_3(t)$;
(3) $\alpha_1 < \alpha < \min\{\alpha_3, \gamma_1(t)\}$ *and* $\beta \in (\alpha, \beta_2)$;
(4) $\alpha_3 < \alpha < \alpha_1 < \gamma_1(t)$ *and* $\beta \in (\alpha, \beta_6)$;
(5) $\max\{\alpha_1, \alpha_3\} < \alpha < \gamma_1(t)$ *and* $\beta \in (\alpha, \min\{\beta_2, \beta_6\}) \cup (\max\{\beta_2, \beta_6\}, 1)$;
(6) $t_2 < \sigma_1 t$, $\alpha < \min\{\alpha_1, \gamma_1(t)\}$ *or* $\alpha_1 < \alpha < \gamma_1(t)$ *and* $\beta \in (\alpha, \beta_2)$;
(ii3) $\sigma_1 t < t_2 < 1$,
(1) $\max\{\alpha_3, \gamma_1(t)\} < \alpha < \gamma_3(t)$ *and* $\beta \in (\beta_6, 1)$;
(2) $\alpha_3 \geq \gamma_3(t)$ *and* $\alpha < \min\{\alpha_1, \gamma_1(t)\}$;
(3) $\alpha_3 \geq \gamma_3(t)$, $\alpha_1 < \alpha < \gamma_1(t)$ *and* $\beta \in (\alpha, \beta_2)$;
(4) $\alpha < \min\{\alpha_3, \gamma_1(t)\}$, $\alpha_1 \geq \gamma_1(t)$ *and* $\alpha_3 < \gamma_3(t)$;

(5) $\alpha_3 < \gamma_3(t)$, $\alpha_3 < \alpha < \gamma_1(t) \le \alpha_1$ *and* $\beta \in (\alpha, \beta_6)$.

In summary, our analysis has elucidated the modulation of individual fluxes J_1 and J_2 by a small positive permanent charge. The effect is determined by the sign of the first-order term J_{k1}: A positive value enhances the flux, and a negative value reduces it. By comparing the critical potentials V_{kc}^1 and V_{kc}^2, we partitioned the voltage into distinct intervals. This allowed us to characterize precisely how the permanent charge influences individual fluxes J_k within each potential interval.

2.2. The impact of permanent charges on $|J_k|$

In this subsection, we investigate how permanent charges influence $|J_k|$, as determined by the sign of $J_{k0}J_{k1}$, under the constraints of boundary conditions (σ, L_k, R_k) and channel geometry (α, β).

Theorem 2.4. *Assume $t = \frac{L_1}{R_1}$. The modulation of individual fluxes by a small positive Q_0 are characterized as follows, depending on the order of the critical potentials V_{1c}^2 and V_{2c}^2:*

(i) $V_{1c}^2 > V_{2c}^2$ *under one of the following conditions:*

(1) $\alpha \ge \gamma_1(t)$;

(2) $\sigma_1 t > 1$, $\alpha < \gamma_1(t)$, *and* $\beta \in (\beta_1, 1)$;

(3) $\sigma_1 t < 1$, $\alpha_1 < \alpha < \gamma_1(t)$, *and* $\beta \in (\beta_2, 1)$.

Under this ordering, the effect of Q_0 is:

(a) *For $V < V_{2c}^2$, Q_0 reduces both $|J_1|$ and $|J_2|$.*

(b) *For $V_{2c}^2 < V < V_{1c}^2$, Q_0 reduces $|J_1|$ but enhances $|J_2|$.*

(c) *For $V > V_{1c}^2$, Q_0 enhances both $|J_1|$ and $|J_2|$.*

(ii) $V_{1c}^2 < V_{2c}^2$ *under one of the following conditions:*

(1) $\sigma_1 t > 1$, $\alpha < \gamma_1(t)$, *and* $\beta \in (\alpha, \beta_1)$;

(2) $\sigma_1 t < 1$ *and* $\alpha < \min\{\alpha_1, \gamma_1(t)\}$;

(3) $\sigma_1 t < 1$, $\alpha_1 < \alpha < \gamma_1(t)$, *and* $\beta \in (\alpha, \beta_2)$.

Under this ordering, the effect of Q_0 is:

(a) *For $V < V_{1c}^2$, Q_0 enhances both $|J_1|$ and $|J_2|$.*

(b) *For $V_{1c}^2 < V < V_{2c}^2$, Q_0 reduces $|J_1|$ but enhances $|J_2|$.*

(c) *For $V > V_{2c}^2$, Q_0 reduces both $|J_1|$ and $|J_2|$.*

Proof. Direct calculation on (2.3) gives

$$V_{1c}^2 - V_{2c}^2 = -\frac{z_1 \ln \sigma + (z_1 - z_2) \ln t}{z_1 z_2 A_2}.$$

Therefore, a direct application of Lemma 2.3 establishes the order of V_{1c}^2 and V_{2c}^2. Statement (i) is proved below, with the rest following from similar reasoning. By calculation, we have

$$J_{10}J_{11} = \frac{R_1 A_1 (\sigma_1 t - 1)(z_1 V + \ln t)^2}{(z_1 - z_2) \ln^3(\sigma_1 t) H^2(1)} \big(z_2 A_2 V + (1 + \frac{z_2}{z_1 - z_2}(1 - A_2)) \ln \sigma + \ln t \big),$$

$$J_{20}J_{21} = \frac{z_1R_1A_1(\sigma_1 t-1)\big(z_2V+\ln(\sigma t)\big)^2}{z_2(z_1-z_2)\ln^3(\sigma_1 t)H^2(1)}\big(z_1A_2V+\frac{z_1}{z_1-z_2}(1-A_2)\ln\sigma+\ln t\big).$$

If $V_{1c}^2 > V_{2c}^2$, a small positive Q_0 modulates the fluxes as follows:

(i) For $V < V_{2c}^2$, it reduces both $|J_1|$ and $|J_2|$ ($J_{10}J_{11} < 0$, $J_{20}J_{21} < 0$).

(ii) For $V_{2c}^2 < V < V_{1c}^2$, it reduces $|J_1|$ but enhances $|J_2|$ ($J_{10}J_{11} < 0$, $J_{20}J_{21} > 0$).

(iii) For $V > V_{1c}^2$, it enhances both $|J_1|$ and $|J_2|$ ($J_{10}J_{11} > 0$, $J_{20}J_{21} > 0$).

It completes the proof. □

The critical potentials V_{1c}^2 and V_{2c}^2, which balance small permanent charge effects and are experimentally accessible (see Section 4), play a key role in our study. They split the electric potential into three subregions, each exhibiting distinct qualitative behaviors of the individual fluxes $|J_1|$ and $|J_2|$. This framework thus provides an efficient way to control ionic flows and ion species preference through the adjustment of boundary conditions.

2.3. Critical potentials: Electroneutrality vs boundary layers

Our aim in this subsection is to compare the orders of critical potentials: V_{kc}^2 (with boundary layers) and V_q^k (under electroneutrality conditions) identified in [31]. We point out that when $\sigma = 1$, one has $V_{kc}^2 = V_q^k$, where the critical potentials from [31] (Formula (4.8) in Theorem 4.8) are given by:

$$V_q^1 = -\frac{\ln t}{z_2(1-B)}, \quad V_q^2 = -\frac{\ln t}{z_1(1-B)},$$

where

$$B = \frac{\omega_1(\alpha)\omega_1(\beta)\ln t}{(\alpha-\beta)(t-1)^2}\ln\frac{\omega_1(\beta)}{\omega_1(\alpha)},$$
$$\omega_1(\alpha) = (1-\alpha)t+\alpha, \quad \omega_1(\beta) = (1-\beta)t+\beta.$$

For $k = 1, 2$, we have

Theorem 2.5. *As $\beta \to \alpha$, V_{1c}^2(resp. V_{2c}^2) is monotonically increasing(resp. decreasing) in $\sigma > 0$. That is, $V_{1c}^2 \geq V_q^1$(resp. $V_{2c}^2 \leq V_q^2$) for $\sigma \geq 1$ and $V_{1c}^2 < V_q^1$(resp. $V_{2c}^2 > V_q^2$) for $\sigma < 1$.*

Proof. We just prove the monotonicity of V_{1c}^2, and the other can be discussed similarly. As recalled from equation (2.3),

$$V_{1c}^2 = \frac{1}{z_1-z_2}\Big(\ln\sigma - \frac{z_1\ln\sigma+(z_1-z_2)\ln t}{z_2A_2}\Big).$$

By considering V_{1c}^2 as a function of σ, it follows from above that

$$\frac{dV_{1c}^2}{d\sigma} = \frac{1}{\sigma z_2(z_1-z_2)}\frac{g(\beta)}{s^2(\beta)},$$

where $s(\beta)$ are defined in (2.2) and

$$g(\beta) = z_2s^2(\beta)+z_1(\alpha-\beta)(t^*-1)\Big[(\beta-\alpha)(t^*-1)\big((t-1)^2+t\ln^2 t\big)$$

$$+ t^*\big(\omega(\alpha)+\omega(\beta)\big)\ln^2 t^* \ln\frac{\omega(\beta)}{\omega(\alpha)}\Big],$$

with $t^* = \sigma_1 t$. When $\beta \to \alpha$, it is easy to check that

$$\lim_{\beta\to\alpha} g(\beta) = \lim_{\beta\to\alpha} g'(\beta) = 0, \quad \lim_{\beta\to\alpha} g''(\beta) = 2(t^*-1)^2 g_1(\alpha),$$

where

$$\begin{aligned} g_1(\alpha) = {} & z_2\big((1-t^*)\ln t^*\big)^2\alpha^2 + 2z_2(1-t^*)\big((1-t^*)\ln t^* + t^*\ln^2 t^*\big)\alpha \\ & + (z_2-z_1)(t^*-1)^2 + \big(z_1\ln t^* + z_2 t^*\ln t^* + 2z_2(1-t^*)\big)t^*\ln t^*. \end{aligned}$$

Direct calculation shows that $g_1(\alpha)$ is a downward-concave quadratic function in α. Moreover, its discriminant is given by

$$\triangle = 4z_1z_2(t^*-1)^2\big((t^*-1)^2 + t^*\ln^2 t^*\big)\ln^2 t^* < 0.$$

Thus, $g_1(\alpha) < 0$, which implies that $g(\beta) < 0$. Therefore, V_{1c}^2 is monotonically increasing in σ since $\frac{dV_{1c}^2}{d\sigma}$ and $g(\beta)$ have the opposite signs. □

3. Numerical simulations

Aiming to provide an intuitive illustration of our key analytical results, this section presents numerical simulations that determine the critical potentials V_{kc}^2 (with boundary layers) and V_q^k (under electroneutrality conditions), characterizing the influences of boundary layers and permanent charge. Our analysis starts by reformulating the system (1.7)-(1.8) as a system of first order ordinary differential equations. Introducing the variables $u = \varepsilon\dot{\phi}$ and $\tau = x$, for $k = 1, 2$, one has

$$\begin{aligned} & \varepsilon\dot{\phi} = u, \quad \varepsilon\dot{u} = -z_1c_1 - z_2c_2 - Q(x) - \varepsilon\frac{h_x(x)}{h(x)}u, \\ & \varepsilon\dot{c}_k = -z_kc_ku - \varepsilon\frac{J_k}{h(x)}, \quad \dot{J}_k = 0, \quad \dot{\tau} = 1, \end{aligned} \tag{3.1}$$

with boundary conditions

$$\phi(0) = V,\ c_k(0) = L_k; \quad \phi(1) = 0,\ c_k(1) = R_k. \tag{3.2}$$

Then, we simulate system (3.1)-(3.2) with the following parameter values: $z_1 = -z_2 = 1,\ \varepsilon = 0.05,\ L_1 = 2,\ R_1 = 10,\ Q_0 = 0.05,\ a = 0.4,\ b = 0.45,\ r_0 = 0.5$,

$$Q(x) = \begin{cases} 0, & 0 < x < a, \\ Q_0, & a < x < b, \\ 0, & b < x < 1, \end{cases} \quad \text{and} \quad h(x) = \begin{cases} \pi\big(-x + r_0 + a\big)^2, & 0 \le x < a, \\ \pi r_0^2, & a \le x < b, \\ \pi\big(x + r_0 - b\big)^2, & b \le x < 1. \end{cases}$$

With the above setup established, direct calculations lead to

$$\alpha = H(a)/H(1) = 0.3608,\ \beta = H(b)/H(1) = 0.3832,\ \beta_2 = 0.3824,$$

$$\alpha_1 = 0.1024,\ \gamma_1(t) = 0.3715,\ \gamma_2(t) = \gamma_3(t) = 0.9938,$$

from which one has

$$0 < \alpha_1 < \alpha < \gamma_1(t) < \beta_2 < \beta < \gamma_2(t) = \gamma_3(t) < 1, \tag{3.3}$$

for $\sigma = 1.005$ in our numerical simulations. More precisely,

(i) Through numerical simulations, we can determine the electric potential V_{kc}^1 and V_q^{k0} for $k = 1, 2$, and observe the monotonicity of function $J_{k0}(V)$, thereby verifying the content of Lemma 2.1. It is further noted that V_{kc}^1 represents a common zero of $J_{k1}(V)$ under boundary layer conditions, whereas V_q^{k0} corresponds to a common zero of $J_{k1}(V)$ under electroneutrality boundary conditions.

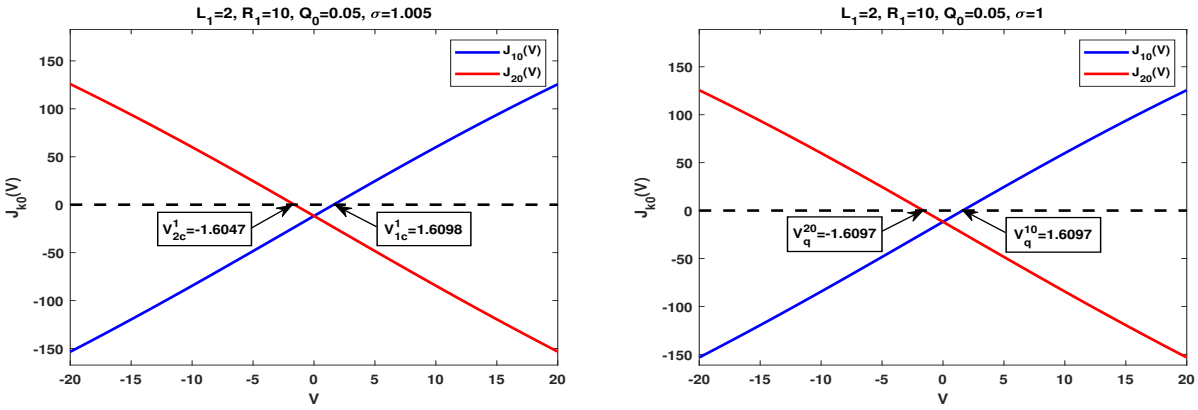

Figure 1. Numerical identifications of V_{kc}^1 and V_q^{k0} for $k = 1, 2$. The monotonicity of the function $J_{k0}(V)$ is shown clearly.

(ii) Under our framework, the inequalities $V_{1c}^1 < V_{1c}^2$ and $V_{2c}^2 < V_{2c}^1$ hold, aligning with statement (i2)(1) in Theorems 2.2 and 2.3, respectively. Moreover, we observe that the function $J_{11}(V)$ is concave upward, while $J_{21}(V)$ is concave downward, which is consistent with the conclusion of Theorem 2.1 (i3), as illustrated in the left panel of Figure 2. It is clear that $V_{kc}^1 \neq V_q^{k0}$ and $V_{kc}^2 \neq V_q^k$, which demonstrates the significant role of boundary layers in the study of ionic flows through membrane channels.

(iii) The inequality $V_{1c}^2 > V_{2c}^2$ is confirmed by our numerical simulations (see the left panel of Figure 3), which is consistent with the analytical result in Theorem 2.4 (i). Furthermore, for $k = 1, 2$,

1. $J_{k0}(V)J_{k1}(V) < 0$ if $V < V_{2c}^2$;
2. $J_{20}(V)J_{21}(V) > 0$ while $J_{10}(V)J_{11}(V) < 0$ if $V_{2c}^2 < V < V_{1c}^2$;
3. $J_{k0}(V)J_{k1}(V) > 0$ if $V > V_{1c}^2$.

That is, a small positive Q_0 modulates the individual fluxes as follows: It reduces both $|J_1|$ and $|J_2|$ for $V < V_{2c}^2$; reduces $|J_1|$ but enhances $|J_2|$ for $V_{2c}^2 < V < V_{1c}^2$; and enhances both $|J_1|$ and $|J_2|$ for $V > V_{1c}^2$. This agrees with our analytical finding in Theorem 2.4 (i).

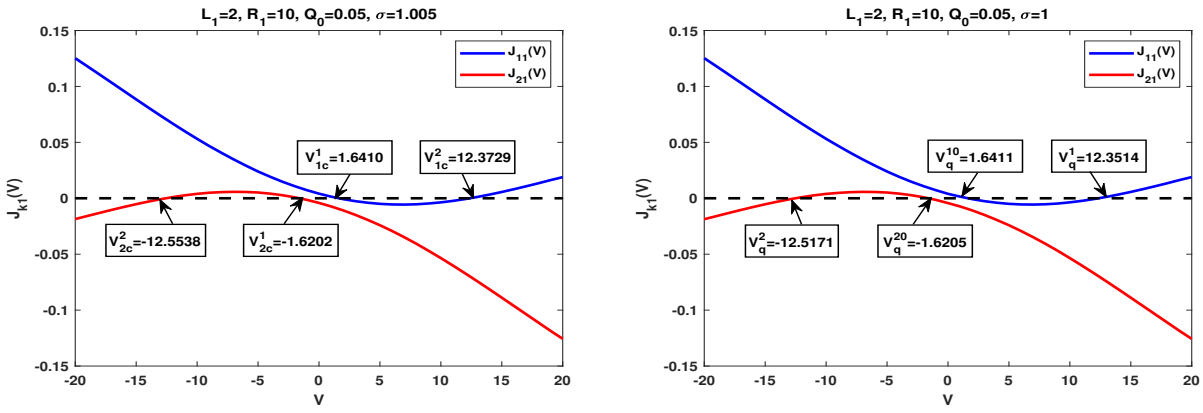

Figure 2. Identification of critical potentials V_{kc}^1, V_{kc}^2 (with boundary layers) and V_q^{k0}, V_q^k (under electroneutrality conditions) for $k = 1, 2$.

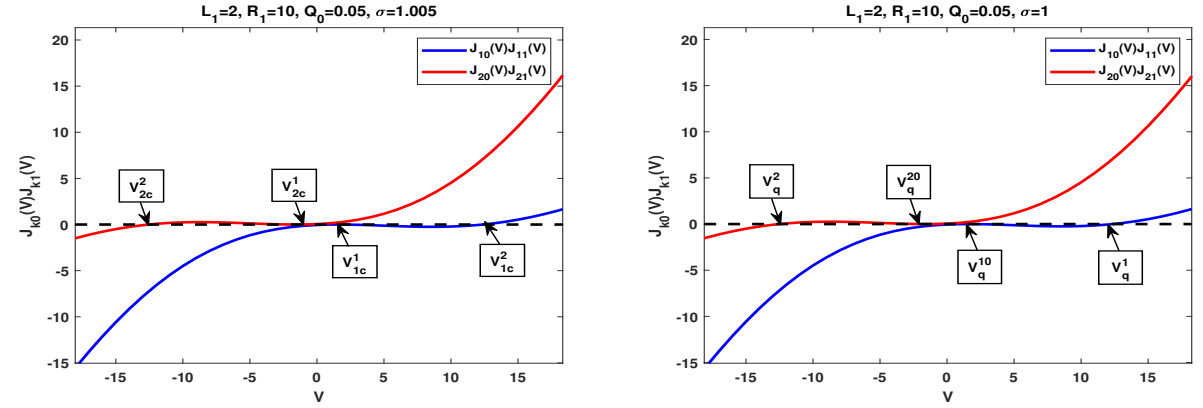

Figure 3. Numerical simulations to $J_{k0}(V)J_{k1}(V)$ under both electroneutrality and non-electroneutrality conditions. The ordering of the critical potentials can be directly observed.

4. Concluding remarks

By analyzing a classical Poisson-Nernst-Planck system with two ion species and small permanent charges, this work examines the combined effects of permanent charge and boundary layers on individual ionic fluxes. In contrast to earlier work [50] that focused on the sign of $J_{k0}J_{k1}$, we emphasize the critical role of J_{k1} itself, the leading-order term that incorporates the influence of small permanent charges and channel geometry. Our results reveal critical potentials that balance the permanent charge effects and play a fundamental role in determining flow properties. The consistency between our numerical simulations and the theoretical analysis provides solid confirmation of the proposed model.

A key contribution of this work lies in its capacity to elucidate the complex interplay among multiple system parameters–including boundary conditions (σ, L_k, R_k), small permanent charges Q_0, and channel geometry (α, β)–in governing individual ion fluxes. Through rigorous analysis, we identify several critical potentials that divide the total region into distinct subregions, each characterized by qualitatively different ionic current behaviors. These results provide essential insights into the underlying mechanisms of ionic flow, particularly its internal dynamics, which are not directly accessible to experimental observation. Importantly, certain of these critical

potentials may be estimated experimentally, thereby offering a promising avenue for bridging theoretical predictions and empirical validation.

In concluding this section, we note that while our model is relatively simple and does not capture the full complexity of crowded ionic mixtures. It was essential for achieving our primary goal: To analyze the specific effects of small permanent charges. This approach is well-justified in contexts like semiconductor problems and synthetic channels, providing a critical first step toward more realistic models. The analytical insights gained, particularly the explicit expressions for ionic fluxes, establish a foundational framework for future research and the development of more complex theories.

Acknowledgments

Both authors thank Prof. Mingji Zhang from New Mexico University, USA for helpful discussions.

References

[1] N. Abaid, R. S. Eisenberg and W. Liu, *Asymptotic expansions of I-V relations via a Poisson-Nernst-Planck system*, SIAM J. Appl. Dyn. Syst., 2008, 7, 1507–1526.

[2] R. Aitbayev, P. W. Bates, H. Lu, L. Zhang and M. Zhang, *Mathematical studies of Poisson-Nernst-Planck systems: Dynamics of ionic flows without electroneutrality conditions*, J. Comput. Appl. Math., 2019, 362, 510–527.

[3] V. Barcilon, *Ion flow through narrow membrane channels: Part I*, SIAM J. Appl. Math., 1992, 52, 1391–1404.

[4] V. Barcilon, D.-P. Chen and R. S. Eisenberg, *Ion flow through narrow membrane channels: Part II*, SIAM J. Appl. Math., 1992, 52, 1405–1425.

[5] V. Barcilon, D.-P. Chen, R. S. Eisenberg and J. W. Jerome, *Qualitative properties of steady-state Poisson-Nernst-Planck systems: Perturbation and simulation study*, SIAM J. Appl. Math., 1997, 57, 631–648.

[6] P. W. Bates, J. Chen and M. Zhang, *Dynamics of ionic flows via Poisson-Nernst-Planck systems with local hard-sphere potentials: Competition between cations*, Math. Biosci. Eng., 2020, 17, 3736–3766.

[7] P. W. Bates, Y. Jia, G. Lin, H. Lu and M. Zhang, *Individual flux study via steady-state Poisson-Nernst-Planck systems: Effects from boundary conditions*, SIAM J. Appl. Dyn. Syst., 2017, 16, 410–430.

[8] P. W. Bates, Z. Wen and M. Zhang, *Small permanent charge effects on individual fluxes via Poisson-Nernst-Planck models with multiple cations*, J. Nonlinear Sci., 2021, 33, 1–62.

[9] D. Boda, D. Busath, B. Eisenberg, D. Henderson and W. Nonner, *Monte Carlo simulations of ion selectivity in a biological Na+ channel: Charge-space competition*, Phys. Chem. Chem. Phys., 2002, 4, 5154–5160.

[10] D.-P. Chen and R. S. Eisenberg, *Charges, currents and potentials in ionic channels of one conformation*, Biophys. J., 1993, 64, 1405–1421.

[11] J. Chen, Y. Wang, L. Zhang and M. Zhang, *Mathematical analysis of Poisson-Nernst-Planck models with permanent charges and boundary layers: Studies on individual fluxes*, Nonlinearity, 2021, 34, 3879–3906.

[12] B. Eisenberg, *Ion channels as devices*, J. Comput. Electro., 2003, 2, 245–249.

[13] B. Eisenberg, *Proteins, channels, and crowded ions*, Biophysical Chemistry, 2003, 100, 507–517.

[14] B. Eisenberg and W. Liu, *Poisson-Nernst-Planck systems for ion channels with permanent charges*, SIAM J. Math. Anal., 2007, 38, 1932-1966.

[15] B. Eisenberg, W. Liu and H. Xu, *Reversal charge and reversal potential: Case studies via classical Poisson-Nernst-Planck models*, Nonlinearity, 2015, 28, 103–128.

[16] R. S. Eisenberg, *Channels as enzymes*, J. Memb. Biol., 1990, 115, 1–12.

[17] R. S. Eisenberg, *Atomic biology, electrostatics and ionic channels*, in New Developments and Theoretical Studies of Proteins, R. Elber, Editor, World Scientific, Philadelphia, 1996, 269–357.

[18] D. Gillespie, *A Singular Perturbation Analysis of the Poisson-Nernst-Planck System: Applications to Ionic Channels*, Ph.D Dissertation, Rush University at Chicago, 1999.

[19] D. Gillespie and R. S. Eisenberg, *Modified Donnan potentials for ion transport through biological ion channels*, Phys. Rev. E, 2001, 63, 061902.

[20] D. Gillespie, W. Nonner and R. S. Eisenberg, *Coupling Poisson-Nernst-Planck and density functional theory to calculate ion flux*, J. Phys. Condens. Matter, 2002, 14, 12129–12145.

[21] D. Gillespie, W. Nonner and R. S. Eisenberg, *Density functional theory of charged, hard-sphere fluids*, Phys. Rev. E, 2003, 68, 0313503.

[22] D. Gillespie, L. Xu, Y. Wang and G. Meissner, *(De)constructing the Ryanodine receptor: Modeling ion permeation and selectivity of the Calcium release channel*, J. Phys. Chem. B, 2005, 109, 15598–15610.

[23] A. L. Hodgkin and R. D. Keynes, *The potassium permeability of a giant nerve fibre*, J. Physiol., 1955, 128, 61–88.

[24] U. Hollerbach, D.-P. Chen and R. S. Eisenberg, *Two- and three-dimensional Poisson-Nernst-Planck simulations of current flow through Gramicidian-A*, J. Comput. Sci., 2002, 16, 373–409.

[25] J. Huang, S. Li and Z. Yao, *Local well-posedness to the free boundary problem of incompressible Euler-Poisson-Nernst-Planck system*, J. Differ. Equations, 2025, 429, 157–203.

[26] Y. Hyon, B. Eisenberg and C. Liu, *A mathematical model for the hard sphere repulsion in ionic solutions*, Commun. Math. Sci., 2010, 9, 459–475.

[27] Y. Hyon, J. Fonseca, B. Eisenberg and C. Liu, *Energy variational approach to study charge inversion (layering) near charged walls*, Discrete Contin. Dyn. Syst. Ser. B, 2012, 17, 2725–2743.

[28] Y. Hyon, C. Liu and B. Eisenberg, *PNP equations with steric effects: A model of ion flow through channels*, J. Phys. Chem. B, 2012, 116, 11422–11441.

[29] S. Ji, B. Eisenberg and W. Liu, *Flux ratios and channel structures*, J. Dyn. Differ. Equ., 2019, 31, 1141–1183.

[30] S. Ji and W. Liu, *Poisson-Nernst-Planck systems for ion flow with density functional theory for hard-sphere potential: I-V relations and critical potentials. Part I: Analysis*, J. Dyn. Differ. Equ., 2012, 24, 955–983.

[31] S. Ji, W. Liu and M. Zhang, *Effects of (small) permanent charges and channel geometry on ionic flows via classical Poisson-Nernst-Planck models*, SIAM J. Appl. Math., 2015, 75, 114–135.

[32] Y. Jia, W. Liu and M. Zhang, *Qualitative properties of ionic flows via Poisson-Nernst-Planck systems with Bikerman's local hard-sphere potential: Ion size effects*, Discrete Contin. Dyn. Syst. Ser. B, 2016, 21, 1775–1802.

[33] G. Lin, W. Liu, Y. Yi and M. Zhang, *Poisson-Nernst-Planck systems for ion flow with density functional theory for local hard-sphere potential*, SIAM J. Appl. Dyn. Syst., 2013, 12, 1613–1648.

[34] W. Liu, *Geometric singular perturbation approach to steady-state Poisson-Nernst-Planck systems*, SIAM J. Appl. Math., 2005, 65, 754–766.

[35] W. Liu, *One-dimensional steady-state Poisson-Nernst-Planck systems for ion channels with multiple ion species*, J. Differ. Equations, 2009, 246, 428–451.

[36] W. Liu, X. Tu and M. Zhang, *Poisson-Nernst-Planck systems for ion flow with density functional theory for hard-sphere potential: I-V relations and critical potentials. Part II: Numerics*, J. Dyn. Differ. Equ., 2012, 24, 985–1004.

[37] W. Liu and B. Wang, *Poisson-Nernst-Planck systems for narrow tubular-like membrane channels*, J. Dyn. Differ. Equ., 2010, 22, 413–437.

[38] W. Liu and H. Xu, *A complete analysis of a classical Poisson-Nernst-Planck model for ionic flow*, J. Differ. Equations, 2015, 258, 1192–1228.

[39] H. Lu, J. Li, J. Shackelford, J. Vorenberg and M. Zhang, *Ion size effects on individual fluxes via Poisson-Nernst-Planck systems with Bikerman's local hard-sphere potential: Analysis without electroneutrality boundary conditions*, Discrete Contin. Dyn. Syst. Ser. B, 2018, 23, 1623–1643.

[40] M. Lv and B. Lu, *A flux-based moving mesh method applied to solving the Poisson-Nernst-Planck equations*, J. Comput. Phys., 2024, 513.

[41] H. Mofidi, F. Hadadifard and M. Zhang, *Analysis of flux-ratio bifurcation in ionic flows via classical Poisson-Nernst-Planck models*, Stud. Appl. Math., 2025, 115, 2.

[42] W. Nooner and R. S. Eisenberg, *Ion permeation and glutamate residues linked by Poisson-Nernst-Planck theory in L-type Calcium channels*, Biophys. J., 1998, 75, 1287–1305.

[43] J.-K. Park and J. W. Jerome, *Qualitative properties of steady-state Poisson-Nernst-Planck systems: Mathematical study*, SIAM J. Appl. Math., 1997, 57, 609–630.

[44] Z. Schuss, B. Nadler and R. S. Eisenberg, *Derivation of Poisson and Nernst-Planck equations in a bath and channel from a molecular model*, Phys. Rev. E, 2001, 64, 1–14.

[45] A. Singer, D. Gillespie, J. Norbury and R. S. Eisenberg, *Singular perturbation analysis of the steady-state Poisson-Nernst-Planck system: Applications to ion channels*, European J. Appl. Math., 2008, 19, 541–560.

[46] A. Singer and J. Norbury, *A Poisson-Nernst-Planck model for biological ion channels–an asymptotic analysis in a three-dimensional narrow funnel*, SIAM J. Appl. Math., 2009, 70, 949–968.

[47] N. Sun and W. Liu, *Flux ratios for effects of permanent charges on ionic flows with three ion species: New phenomena from a case study*, J. Dyn. Differ. Equ., 2024, 36, 27–62.

[48] N. Sun and W. Liu, *Flux ratios for effects of permanent charges on ionic flows with three ion species: A universality (III)*, J. Differ. Equations, 2025, 421, 264–290.

[49] X.-S. Wang, D. He, J. Wylie and H. Huang, *Singular perturbation solutions of steady-state Poisson-Nernst-Planck systems*, Phys. Rev. E, 2014, 89, 022722.

[50] Y. Wang, L. Zhang and M. Zhang, *Studies on individual fluxes via Poisson-Nernst-Planck models with small permanent charges and partial electroneutrality conditions*, J. Appl. Anal. Comput., 2022, 12, 87–105.

[51] Z. Wen, P. Bates and M. Zhang, *Effects on I-V relations from small permanent charge and channel geometry via classical Poisson-Nernst-Planck equations with multiple cations*, Nonlinearity, 2021, 34, 4464–4502.

[52] Z. Wen, L. Zhang and M. Zhang, *Dynamics of classical Poisson-Nernst-Planck systems with multiple cations and boundary layers*, J. Dyn. Differ. Equ., 2021, 33, 211–234.

[53] M. Zhang, *Asymptotic expansions and numerical simulations of I-V relations via a steady-state Poisson-Nernst-Planck system*, Rocky MT. J. Math., 2015, 45, 1681–1708.

[54] M. Zhang, *Boundary layer effects on ionic flows via classical Poisson-Nernst-Planck systems*, Comput. Math. Biophys., 2018, 6, 14–27.

Received December 2025; Accepted March 2026; Available online March 2026.